UDK 669.35'6:620.193
Original scientific article/Izvirni znanstveni članek

ISSN 1580-2949
MTAEC9, 45(6)585(2011)

CORROSION STABILITY OF DIFFERENT BRONZES IN SIMULATED URBAN RAIN

KOROZIJSKA STABILNOST RAZLIČNIH BRONOV V UMETNEM KISLEM DEŽJU

Erika Švara Fabjan, Tadeja Kosec, Viljem Kuhar, Andraž Legat

National Building and Civil Engineering Institute, Dimičeva 12, 1000 Ljubljana, Slovenia
erika.svara@zag.si

Prejem rokopisa – received: 2011-04-16; sprejem za objavo – accepted for publication: 2011-06-06

Copper and high copper alloys tend to passivate in humid air. In clean humid air, cuprite slowly transforms to black tenorite. If atmosphere contains aggressive species, acid rain might effect the formation of different corrosion products. The patina that forms upon exposure to urban acid rain also depends of the composition of the base alloy. In the present study three different alloys were investigated: leaded bronze, usually used for sculptures, unleaded bronze as an alloy without an impact on the environment, and new type of bronze alloy, silicon bronze.
The electrochemical measurements were performed to investigate the different bronze properties in simulated urban acid rain that contained carbonates, sulphates and nitrates, acidified to pH 5. Morphological characteristics of the three different bronzes were studied and SEM/EDX analysis of the corrosion products was performed.
It was found that silicon bronze has higher corrosion resistivity than unleaded bronze, the former having higher corrosion resistivity than leaded bronze. In addition, time dependant electrochemical impedance spectroscopy measurements showed that polarization resistances for silicon bronze and unleaded increased with time, whereas it decreased for leaded bronze. The corrosion layer on silicon bronze is more compact and thinner due to homogeneous microstructure.

Keywords: bronze, metallography, corrosion, simulated urban rain

Baker ter bakrove zlitine se na vlažnem zraku pasivirajo, prihaja do nastanka t. i. patin. Najprej se tvori rdečkast kuprit, ki se nato počasi spreminja v črn tenorit. Če pa so v atmosferi agresivne zvrsti, lahko nastali kisli dež vpliva na tvorbo različnih korozijskih produktov. Patina, ki se tvori zaradi izpostavitve kislemu dežju, je odvisna tudi od sestave zlitine. V študiji smo preiskovali tri različne vrste bronastih zlitin: bron z vsebnostjo svinca, pogosto uporabljen pri ulivanju večjih bronastih spomenikov, bron brez vsebnosti svinca ter novo vrsto brona s silicijem.
Elektrokemijske preiskave smo izvedli v simulirani raztopini kislega dežja, ki je vsebovala sulfate, karbonate in nitrate. Določili smo mikrostrukturne značilnosti posameznih bronov ter morfologijo korozijskih produktov.
Ugotovili smo, da je najbolj korozijsko odporna zlitina bakra s silicijem, sledi recentna zlitina brez svinca, najslabše korozijske lastnosti pa ima zlitina s svincem. Nadalje smo z elektrokemijsko impedančno spektroskopijo pokazali, da se korozijske lastnosti zlitine s svincem s časom slabšajo, korozijske lastnosti zlitine brez svinca ter bron s silicijem pa se s časom izboljšujejo. Korozijski produkti na silicijevi zlitini so kompaktni predvsem zaradi homogene mikrostrukture.

Ključne besede: bron, metalografija, korozija, simulirana raztopina kislega dežja

1 INTRODUCTION

Copper and copper alloys may corrode different ways depending on the type of atmosphere that the bronze objects are exposed to. In rural areas where atmosphere is clean, the bronze surface first turns reddish forming cuprite and finally it transforms to black tenorite. In general, urban and marine atmosphere are more aggressive, and versatile corrosion products form on non protected copper or bronze. Numerous studies have been involved in the subject [1–28].

The bronze problematics is very wide in its area, it covers studies of different bronze types [3,7,11,20] and natural patinas that form on copper or bronze [1,8–10,19,24,25,28]. The main concern in some studies is protection of natural and synthetic artificial patinas [4,5,14,15,18,19]. Much work is devoted to different corrosion inhibitors [5,14,16–18,27] next to different basic electrochemical studies [6,22,23].

The corrosion products that form in particular type of bronze are strongly dependant on the type of bronze, the type of the atmosphere, the chemical and physical preparation of surface, patinations and protections. The two scientific works were result of EUREKA– 2210 Eurocare bronzart project, where different cast bronzes for production of bronze artworks were studied [7,11].

The seven different types of bronze with different contents of copper, tin, zinc, lead, silicon and nickel were employed in the study by Gallese et al. [11]. It was shown that the bronze alloy with minimal content of Pb (Cu–4Sn–5Zn) showed very good characteristics, as well as the bronze alloy with less zinc and more tin (Cu–9Sn–1.5 Zn) and alloy with the presence of Ni (Cu–9Sn–2Zn–3Ni). All these alloys showed improved corrosion characteristics when compared to reference alloy (Cu–5Sn–4Zn–5Pb). This traditional alloy that contains lead is recognized as problematic due to lead toxicity.

In another study, the electrochemical properties of alloy Cu–5Sn–5Zn–5Pb (G85) were compared to SI3 (Cu–8Sn–3Si) in simulated acid rain and the corrosion characteristics were evaluated after exposure in simulated urban–industrial and marine environment. It was found out that silicon bronze exhibited better corrosion resistance in more aggressive marine environment [7].

It is of big importance to develop and investigate bronzes that would perform well in different corrosive environments. The information could provide more knowledge and appropriate selection of suitable materials for the application in the field of Cultural Heritage. The selection of proper alloy in different environments could be improved to minimize visual change of bronze surface as well as unwanted appearance of corrosion products. Novelty feature of this study is the evaluation of the difference in corrosion performance of older and newer type of alloys.

The main objectives of the present study were to electrochemically investigate the difference of the three different bronze types: Cu–Zn–Sn and Cu–Zn–Sn–Pb and Cu–Sn–Si. Potentiodynamic techniques as well as electrochemical impedance spectroscopy were used for the study of electrochemical behaviour and passive layers that formed in simulated urban rain at open circuit potential. The morphological examination was performed. The SEM/EDX spectroscopic investigation was made in order to examine the corrosion products that had formed during 35 days immersion in simulated urban rain solution.

2 EXPERIMENTAL

2.1 Material and surface preparation

The bronze samples were cast in a sand mould of dimension of (100 × 100 × 5) mm. Three different bronzes were chosen to be investigated: CuSnZn, CuSnZnPb and CuSnSi. CuSnZn bronze is currently used for casting of big bronze sculptures, bronze CuSnZnPb contains some lead, which is advised to be omitted in newly casted sculptures, and new type of bronze that contains silicon: CuSnSi. The composition of the three different bronzes, determinated by portable X-ray fluorescence analysers X-MET5100, Oxford Instruments, UK, is given in **Table 1**.

Samples were sectioned from 5 mm plates in the form of discs of 15 mm diameter used as working electrodes. Prior to measurement, the specimens were abraded with 800 and 1000 grid emery paper. Finally, the samples were ultrasonically cleaned in distilled water and then well dried.

2.2 Electrochemical measurements

The electrochemical measurements were performed in a solution of 0.2 g/L Na_2SO_4, 0.2 g/L $NaHCO_3$ and 0.2 g/L $NaNO_3$. It was acidified with H_2SO_4 to pH 5 in order to simulate the acid rain which is frequently found in polluted urban environments (this atmosphere was designated: "simulated urban rain"). Four different electrochemical measurements were done for three different types of bronzes.

A three–electrode corrosion cell was used with a volume of 350 cm^3. The working electrode was embedded in a Teflon holder, and had an exposed area of 0.785 cm^2. Saturated calomel electrode (SCE, E = 0.2415 V) was used as reference electrode and two stainless steal rods served as a counter electrode. For electrochemical tests a Gamry 600 potentiostat/galvanostat, expanded with a Gamry Instruments framework module was used.

Following initial 1 h stabilization at open circuit potential (OCP), linear polarization measurements at ±20 mV vs. OCP with a scan rate 0.1 mV/s were performed. Finally, electrochemical impedance measurements, the frequency range ranged from 65 kHz to 5 MHz at 10 cycles per decade, with an ac amplitude of ±10 mV, were monitored. The absolute impedance and phase angle were measured at each frequency. The impedance measurements were carried out after different times of immersion (1 h, 4 h, 8 h and 12 h) in the electrolyte. All potentials are reported with respect to the SCE scale.

2.3 SEM/EDX analysis

For SEM/EDX analysis the different alloys were immersed in a simulated urban rain, pH 5 for 35 d under stationary conditions. At the end of exposure, the specimens were taken from the solutions, rinsed with distilled water and dried. Surface morphology was inspected and analyzed with a low vacuum scanning electron microscope (SEM, JSM 5500 LV, JOEL, Japan) at acceleration voltage of 20 kV. The microscope was equipped with energy dispersive spectrometer (Inca, Oxford Instruments Analytical, UK). EDS analysis was performed at an acceleration voltage of 20 kV.

2.4 Metalographic examination

Samples were first grounded up to grades 2000, then they were polished up to 4000 and finally 0.5 μm paste was used. Etching for uncovering the microstructure was performed using solution of ammonium and hydrogen peroxide for 3 min. The sample was then immediately rinsed with alcohol and dried with air.

Table 1: The composition of the three different bronzes in mole fractions, *x*/%
Tabela 1: Sestava različnih bronastih zlitin v molskih deležih, *x*/%

Bronze alloy / Composition	Cu	Sn	Zn	Pb	Si	Al	P	Fe	the rest
CuSnZn	87.0	5.5	3.6	0.1	–	0.6	–	0.1	3.1
CuSnZnPb	87.1	6.6	1.1	5.0	–	–	0.1	0.1	0
CuSnSi	85.5	9.6	0.1	0.1	2.5	–	0.1	0.1	2.0

A CARL ZEISS AXIO Imager M2m optical metallographic microscope was used to inspect the microstructure of specimens. Metallographic specimens were prepared and investigated in the longitudinal and transverse direction of castings.

3 RESULTS AND DISCUSSION

3.1 Metalographic examination

Unleaded bronze, CuZnSn, revealed a non–homogeneous material consisting of dendrites of β–tin and zinc eutectics in the matrix of α–copper. CuSnZn bronze many microstructural imperfections, such as shrinkage cavities, pores and non–uniform dendrite distribution (**Figure 1a and 1b**).

Microstructure of CuSnZnPb bronze consisted of similar eutectics and matrix as CuSnZn bronze. Lead produced by the eutectic reaction was distributed inter–dendritically in copper as small globules. Some shrinkage cavities (black inter–dendritic network) could be observed in the microstructure (**Figure 1c and 1d**).

Silicon bronze, denoted as CuSnSi, is a very homogeneous material in both longitudinal and transverse direction (**Figure 1e and 1f**). It consisted of dendrites of silicon and β–tin eutectics in matrix of α–copper. It was reported that higher tin content in the alloy might improve corrosion resistance of the bronze [7].

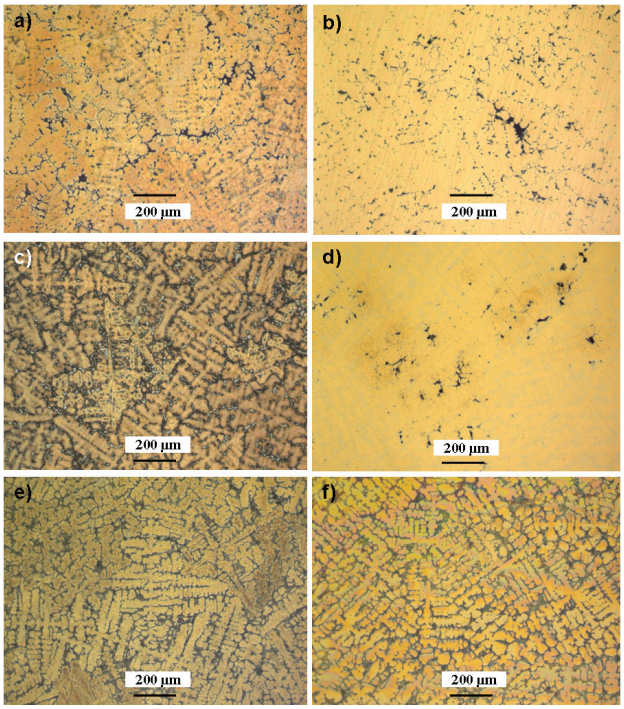

Figure 1: Metalographic images of the three different bronzes (CuSnZnPb– a and b, CuSnSi–c and d and CuSnZn– e and f), exposed surface direction–longitudinal (a, c, e) and cross–sections–transverse side (b, c, f). All shown images are etched, except b) and f), which are polished.

Slika 1: Metalografski posnetki treh različnih vrst brona (CuSnZnPb– a in b, CuSnSi–c in d ter CuSnZn– e in f). Longitudinalna smer je izpostavljena površina brona (a, c, e) in prerez brona (b, c, f). Broni na prikazanih posnetkih so jedkani, razen na posnetkih b) in f), kjer je prikazana brušena površina.

3.2 Electrochemical measurements

In order to evaluate corrosion properties of the three different bronzes, electrochemical experiments were conducted in a simulated urban rain, pH 5. For further evaluation of corrosion behaviour, the samples were immersed in the simulated urban rain solution for 35 d. After that, the surface was examined by EDX/SEM technique.

3.2.1 Open circle potential measurement

During the stabilization process, the open circuit potential was measured as a function of time. **Figure 2** represents open circuit potential curves of all three investigated bronzes, immersed in the urban rain solution with pH 5. All curves show a similar electrochemical behaviour. The corrosion potential, E_{OC} at the beginning of exposure (up to 500 s) did not change much with time for CuSnZn and CuSnSi. For leaded bronze CuSnZnPb it moved to slightly more positive values at the beginning of exposure. Then, the corrosion potential in all cases moved to more negative values of potentials. After one hour of immersion it stabilized at –0.025 V for bronze CuSnZn and at a slightly more positive potential for bronze CuSnZnPb at –0.020 V. Corrosion potential for CuSnSi stabilized at –0.030 V after 1 h of immersion. The observed decrease of the value of E_{OC} in time might be a result of formation of adsorbed layer at interface bronze/electrolyte due to carbonate, sulphate and nitrate ions in simulated urban rain. However, *E*oc evolution is quite regular, indicating a stable process occurring through a relative stable layers that formed on investigated bronze surfaces.

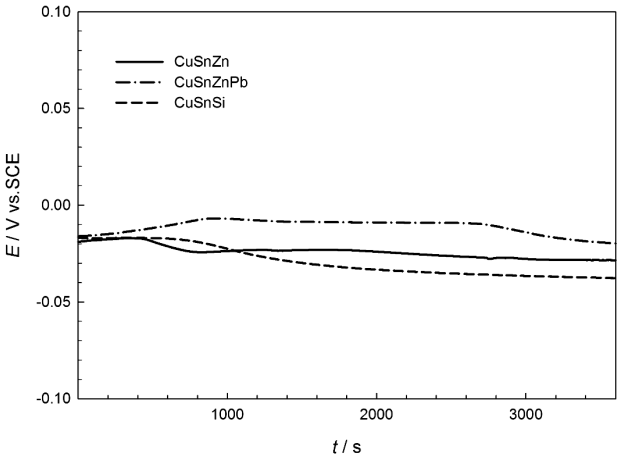

Figure 2: Open circuit potential measurements for the three different bronzes: CuSnZn, CuSnZnPb and CuSnSi, immersed in simulated urban rain solution, pH 5.

Slika 2: Meritve pri potencialu odprtega kroga za tri različne brone CuSnZn, CuSnZnPb in CuSnSi, potopljene v simulirano raztopino mestnega dežja, pH 5.

3.2.2 Polarization resistance (R_p) measurements

One hour after immersion of CuSnZn, CuSnZnPb and CuSnSi in simulated urban rain, pH 5, the linear polarization measurements at a scan rate of 0.1 mV/s were executed (**Figure 3**). The slope of the curve potential–current is the polarization resistance value as described in Stearn Geary equation (1):

$$R_{\mathrm{p}(\Delta E \to 0)} = \frac{\Delta E}{\Delta j} \quad (1)$$

The average measured values for the three bronzes are presented in **Table 2**. The lowest value of polarization resistance (R_p = 2.3 kΩ cm^2) corresponded to leaded bronze, CuSnZnPb and the highest value of polarization resistance corresponded to silicon bronze, CuSnZnSi (R_p = 4.6 kΩ cm^2). The lowest value of polarization resistance for CuSnZnPb exhibited the highest corrosion susceptibility of leaded bronze, whereas values for Silicon bronze CuSnSi showed higher corrosion resistance in simulated urban rain than leaded bronze and bronze CuSnZn. Similar observation was found by Chiavari and coworkers [7]. In their study, leaded bronze and silicon bronze exhibited similar electrochemical behaviour at initial stages but after 7 d, the corrosion rate of leaded bronze was decreased. It was ascribed to formation of uniform and stable passive layer on silicon bronze in comparison with passive layer on leaded bronze. Namely, the passive layer on silicon bronze hindered the oxygen diffusion to the copper surface.

3.2.3 Electrochemical impedance spectroscopy (EIS) measurements

Figure 4 represents the Nyquist diagrams for the three different bronze samples: CuSnZn, CuSnZnPb and CuSnSi at different immersion times during 12 h of immersion in simulated urban rain solution with pH 5.

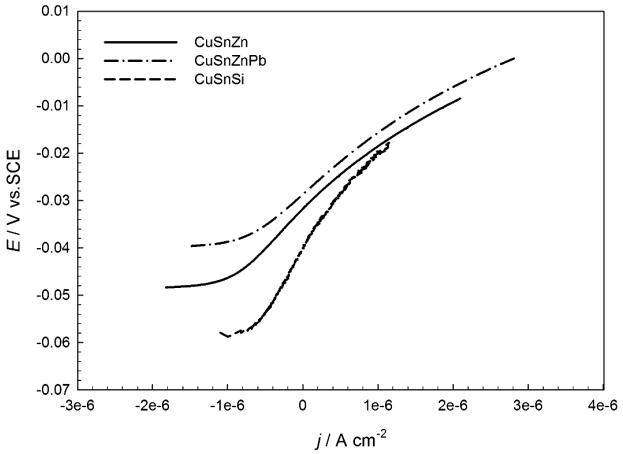

Figure 3: Polarization resistance curves for CuSnZn, CuSnZnPb and CuSnSi immersed in simulated urban rain, pH 5 at a scan rate 0.1 mV/s

Slika 3: Meritve linearne upornosti za CuSnZn, CuSnZnPb in CuSnSi, potopljene v simulirano raztopino mestnega dežja, pH 5, pri hitrosti preleta 0,1 mV/s

Table 2: Corrosion potential, E_{corr} and polarization resistance values, R_p, deduced from linear polarization measurements

Tabela 2: Korozijski potencial E_{kor} in vrednosti polarizacijskih upornosti R_p, dobljenih iz meritev linearne upornosti

Material	E_{corr} /V	R_p/(kΩ cm^2)
CuSnZn	–0.032	3.2
CuSnZnPb	–0.029	2.3
CuSnSi	–0.038	4.6

Table 3: The estimated polarization resistance from EIS measurements in dependence of the time, values of R_p/(kΩ cm^2)

Tabela 3: Ocenjene vrednosti polarizacijskih upornosti iz meritev EIS v različnih časovnih obdobjih R_p/(kΩ cm^2)

Immersion time	1 h	4 h	8 h	12 h
$R_{p\ (CuSnZn)}$	15	13	23	25
$R_{p\ (CuSnZnPb)}$	3.4	3.4	3.1	2.9
$R_{p\ (CuSnSi)}$	5.2	5.0	5.9	9.2

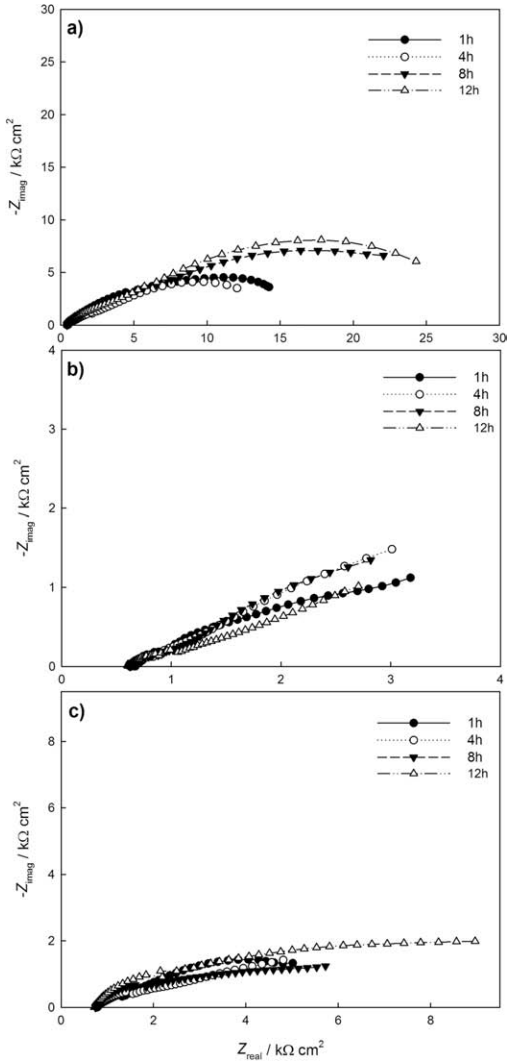

Figure 4: EIS response as Nyquist plots for different bronzes: a) CuSnZn, b) CuSnZnPb and c) CuSnSi after different immersion times in a simulated urban rain solution, pH 5.

Slika 4: EIS-odziv v obliki Nyquistovih diagramov za različne brone CuSnZn, CuSnZnPb in CuSnSi po različnih časih potopitve v simulirano raztopino mestnega dežja, pH 5.

Nyquist diagram corresponding to bronze CuSnZn was characterized by high frequency intercept at the abscise axis and broad and semi-depressed loop at lower frequencies (**Figure 3**). One time constant was observed at 1 h immersion which then evolves with two clearly resolved time constants at 12 h immersion time. Estimated polarization resistances (R_p) were determinated from impedance modulus at the lowest value of frequencies, as presented in **Table 3**. During 12 h immersion, impedance values for bronze CuSnZn increased with time. Thus, the estimated polarization resistance increased with immersion time. Stable layer of protective products had formed.

The Nyquist diagram for CuSnZnPb (**Figure 4**) was characterized by high frequency intercept at the absise axis, broad depressed loop at middle frequencies and straight line at low frequencies. The high frequency intercept is relatively high due to low conductivity of the urban acid rain solution. The shape of impedance response indicated the undefined time constant as observed from Bode diagrams (not shown). Also, the phase shift is very low for all times of immersion. Impedance response is not highly dependant of the immersion time, but a slight decrease is observed, as also presented in **Table 3**. Nyquist diagram for CuSnSi showed similar impedance behaviour to the sample CuSnZn including similar diagram shape and increasing value of impedance response. Also, the estimated polarization resistance value increased with immersion time (**Table 3**).

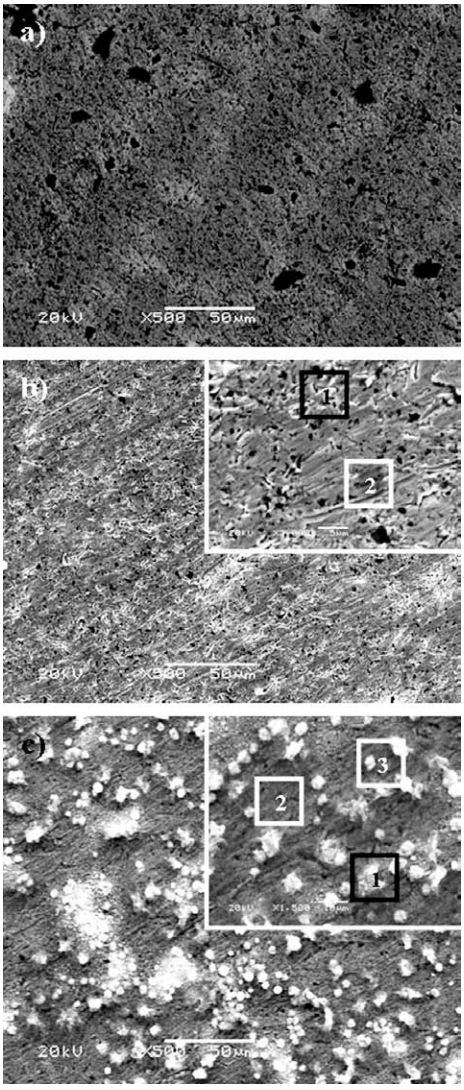

Figure 5: SEM image of a) CuSnZn b) CuSnZnPb and c) CuSnSi after 35 d of immersion in simulated urban rain solution pH 5
Slika 5: SEM-prikaz a) CuSnZn b) CuSnZnPb and c) CuSnSi po 35 d izpostavitve v simulirani raztopini mestnega dežja, pH 5

Thus, our results showed that the corrosion rate of unleaded bronze and silicon bronze decreased with time, whereas corrosion rate for leaded bronze increased with time. Impedance spectroscopy results show that unleaded bronze showed slightly better corrosion characteristics due to bigger estimated polarization resistances when compared to silicon bronze. However, the appearance of silicon bronze corrosion products is favourable over unleaded bronze, as shown in the next chapter of results.

Our results are similar to results reported by Chiavari *et al.* [7]. They investigated the silicon bronze (3 % Si) and leaded bronze (5 % Pb) in acid rain solution pH 3.1 by conducting different electrochemical measurements at different immersion times in acid rain solution pH 3.1. They found out that corrosion rate of silicon bronze decreased after long immersion time due to formation of stable layer of protective corrosion product, whereas in the case of leaded bronze the corrosion rate increased.

3.3 Surface characterization by SEM / EDX analysis

After 35–day immersion in simulated acid rain solution pH 5 under stagnant conditions, the samples of CuSnZn, CuSnZnPb and CuSnSi were examined by Scanning Electron Microscopy (SEM) and quantitatively analysed by EDS analysis (**Figure 5**). Differences of patina formation were observed already with a naked eye (not shown). Patina on unleaded bronze CuSnZn exhibited orange type compact corrosion product, whereas patina on leaded bronze after 35 day immersion in urban acid rain was brown–reddish and uneven. Patina that formed on silicon Bronze CuSnSi looked like smoky brown colour and very compact and thin.

The SEM image of sample CuSnZn after 35 d of exposure to urban acid rain (**Figure 5a**) showed homogeneously coated surface with corrosion products. The EDS analysis indicated the presence of mainly copper, oxygen and carbon (mole fractions x: 41 %, 35 % and 10 %), whereas Zn, Sn, S, Si were present as minor elements. Due to high percentage of oxygen in the analysed layer, the bronze surface presumably contained other corrosion products apart from cuprite, Cu_2O. The possible proposed mineral was brochantite [16]. The SEM image of leaded bronze, CuSnZnPb (**Figure 5b**), after 35 day immersion in acid rain solution exhibited two different

areas, denoted as area No. 1b and area No. 2b. Area No. 1b contained mainly carbon, less oxygen and copper, and nitrogen and lead in trace amounts. That indicated to copper carbonate as possible corrosion product. Whereas darker area, denoted as area No. 2b, was rich in copper (*x*/% : 51 % Cu, 2 % Sn, 27 % C, 9 % N and 11 % O) and contain more tin than area No. 1. The darker area could be the base alloy, not yet entirely covered by corrosion products. Cuprite and SnO_2 were proposed as the most possible oxidation products.

The SEM micrograph of CuSnSi (**Figure 5c**) showed three different areas, denoted as Area No. 1c, Area No. 2c and Area No. 3c. All analysed areas examined contained similar elements but in different ratios. Corrosion products in the shape of white spherical particles (Area No. 1) are rich in oxygen, carbon, nitrogen and sulphur. The formation of sulphates (brohantite $Cu_4SO_4(OH)_6$ or naukarite $Cu_4(SO_4)_4(CO_3)(OH)_6{\cdot}48\ H_2O$) was proposed. Grey coloured area, denoted as Area No.2c, is rich in tin, silicon and copper and less rich in oxygen and sulphur, indicated the formation of SiO_2 and SnO_2. Area No.3c is in composition similar to area No. 1c, but contained less sulphur.

It is difficult to unambiguously differentiate the corrosion products, grown during 35 d immersion in urban acid rain on the three different bronzes as the corrosion layers are too thin to detect the EDS signal just from corrosion products. However, the visual inspection of the patina layers on the three different bronzes showed that the patinas were different as the result of the base alloy composition.

Chiavari et al [7] who studied leaded bronze and silicon bronze in climatic chamber with chlorides and sulphates, showed that the main corrosion product on leaded bronze was brochantite, and that the layer on Silicon bronze was thinner and more compact. Also, similarly to our case, the corrosion products on leaded bronze were more non-homogeneous and thicker.

As the result of microstructural characteristics of the three different bronzes, it can be concluded that surface imperfections, non homogeneous distribution of corrosion products formed in the case of leaded bronze CuSnZnPb. Even distribution of corrosion products on Silicon bronze is also a result of homogeneous distribution of metallographic phases on silicon bronze, whereas unleaded bronze CuSnZn behaved somehow in between.

4 CONCLUSIONS

Three different bronzes were investigated in simulated urban rain solution, pH 5: recent bronze CuSnZn, leaded bronze CuSnZnPb and newer representative of bronzes, silicon bronze CuSnSi.

Microstructural investigation showed that recent bronze CuSnZn consisted of β–tin and zinc eutectics in α–copper. Inter dendritic network of shrinkage cavities were observed as an alloy imperfection. Similar observation occurred for leaded bronze, where lead as globules intermixed in α–copper of the bronze alloy. Silicon bronze has extremely oriented microstructure which is very regular. It consisted of dendrites of silicon and β–tin eutectics in matrix of α–copper.

Electrochemical investigation of different bronzes in simulated urban rain solution showed that the leaded bronze is most likely to corrode the most, followed by recent bronze CuSnZn. The highest corrosion resistivity among the bronzes was found for silicon bronze, CuSnSi.

Time dependence during 12 h immersion was followed by electrochemical impedance spectroscopy measurements. It was showed that corrosion resistance decreased with time for leaded bronze, whereas it increased for unleaded bronze CuSnZn and silicon bronze CuZnSi.

Morphological observation of corrosion products that formed during 35 d immersion in stagnant solution of urban acid rain showed that the patina layer is different for the three different bronzes. It is non–homogeneous for leaded bronze and very thin and compact for silicon bronze. It is believed that alloy composition and micro-structural characteristic have a great impact on electrochemical behaviour and formation of oxidation products–bronze patina layer. It affects visual appearance as well as chemical composition of corrosion products.

Unleaded bronze can successfully replace the use of leaded bronze where also better corrosion characteristics were found. Silicon bronze can be used in environments where only small changes of appearance of corrosion products are expected.

5 REFERENCES

[1] Ammeloot, F.; Fiaud, C.; Sutter, E. M. M., Characterization of the oxide layers on a Cu-13Sn alloy in a NaCl aqueous solution without and with 0.1 M benzotriazole. Electrochemical and photoelectrochemical contributions. Electrochimica Acta, 44 (**1999**) 15, 2549–2558

[2] Bendezu, R. D.; Goncalves, R. P.; Neiva, A. C.; de Melo, H. G., EIS and microstructural characterization of artificial nitrate patina layers produced at room temperature on copper and bronze. Journal of the Brazilian Chemical Society, 18 (**2007**) 1, 54–64

[3] Bernardi, E.; Chiavari, C.; Lenza, B.; Martini, C.; Morselli, L.; Ospitali, F.; Robbiola, L., The atmospheric corrosion of quaternary bronzes: The leaching action of acid rain. Corrosion Science, 51 (**2009**) 1, 159–170

[4] Bierwagen, G.; Shedlosky, T. J.; Stanek, K., Developing and testing a new generation of protective coatings for outdoor bronze sculpture. Progress in Organic Coatings, 48 (**2003**) 2–4, 289–296

[5] Brunoro, G.; Frignani, A.; Colledan, A.; Chiavari, C., Organic films for protection of copper and bronze against acid rain corrosion. Corrosion Science, 45 (**2003**) 10, 2219–2231

[6] Cano, E.; Polo, J. L.; La Iglesia, A.; Bastidas, J. M., Rate control for copper tarnishing. Corrosion Science, 47 (**2005**) 4, 977–987

[7] Chiavari, C.; Colledan, A.; Frignani, A.; Brunoro, G., Corrosion evaluation of traditional and new bronzes for artistic castings. Materials Chemistry and Physics, 95 (**2006**) 2–3, 252–259

[8] Chiavari, C.; Rahmouni, K.; Takenouti, H.; Joiret, S.; Vermaut, P.; Robbiola, L., Composition and electrochemical properties of natural patinas of outdoor bronze monuments. Electrochimica Acta, 52 (**2007**) 27, 7760–7769

[9] Cicileo, G. P.; Crespo, M. A.; Rosales, B. M., Comparative study of patinas formed on statuary alloys by means of electrochemical and surface analysis techniques. Corrosion Science, 46 (**2004**) 4, 929–953

[10] de la Fuente, D.; Simancas, J.; Morcillo, M., Morphological study of 16–year patinas formed on copper in a wide range of atmospheric exposures. Corrosion Science, 50 (**2008**) 1, 268–285

[11] Gallese, F.; Laguzzi, G.; Luvidi, L.; Ferrari, V.; Takacs, S.; Venturi Pagani Cesa, G., Comparative investigation into the corrosion of different bronze alloys suitable for outdoor sculptures. Corrosion Science, 50 (**2008**) 4, 954–961

[12] Hayez, V.; Costa, V.; Guillaume, J.; Terryn, H.; Hubin, A., Micro Raman spectroscopy used for the study of corrosion products on copper alloys: study of the chemical composition of artificial patinas used for restoration purposes. Analyst, 130 (**2005**) 4, 550–556

[13] Hernandez, R. P. B.; Paszti, Z.; de Melo, H. G.; Aoki, I. V., Chemical characterization and anticorrosion properties of corrosion products formed on pure copper in synthetic rainwater of Rio de Janeiro and Sao Paulo. Corrosion Science, 52 (**2010**) 3, 826–837

[14] Marusic, K.; Otmacic–Curkovic, H.; Horvat–Kurbegovic, S.; Takenouti, H.; Stupnisek–Lisac, E., Comparative studies of chemical and electrochemical preparation of artificial bronze patinas and their protection by corrosion inhibitor. Electrochimica Acta, 54 (**2009**), 27, 7106–7113

[15] Muresan, L.; Varvara, S.; Stupnisek–Lisac, E.; Otmacic, H.; Marusic, K.; Horvat–Kurbegovic, S.; Robbiola, L.; Rahmouni, K.; Takenouti, H., Protection of bronze covered with patina by innoxious organic substances. Electrochimica Acta, 52 (**2007**) 27, 7770–7779

[16] Otmačić Ćurković H, Kosec T., Legat A, Stupinšek–Lisac E, Improvement of corrosion stability of patinated bronze. Corrosion Engineering, Science and Technology, 45 (**2010**) 327–333

[17] Otmacic, H.; Stupnisek–Lisac, E., Copper corrosion inhibitors in near neutral media. Electrochimica Acta, 48 (**2003**) 8, 985–991

[18] Rahmouni, K.; Takenouti, H.; Hajjaji, N.; Srhiri, A.; Robbiola, L., Protection of ancient and historic bronzes by triazole derivatives. Electrochimica Acta, 54 (**2009**) 22, 5206–5215

[19] Robbiola, L.; Blengino, J. M.; Fiaud, C., Morphology and mechanisms of formation of natural patinas on archaeological Cu–Sn alloys. Corrosion Science, 40 (**1998**) 12, 2083–2111

[20] Rosales, B. M.; Vera, R. M.; Hidalgo, J. P., Characterisation and properties of synthetic patina on copper base sculptural alloys. Corrosion Science 52 (**2010**) 10, 3212–3224

[21] Schweitzer, P. A., Fundamentals of metallic corrosion : Atmosferic and Media Corrosion of Metals, Corrosion Engineering Handbook, 2nd Ed. RC Press/Taylor & Francis Group: Boca Raton, FL., 2007

[22] Serghini–Idrissi, M.; Bernard, M. C.; Harrif, F. Z.; Joiret, S.; Rahmouni, K.; Srhiri, A.; Takenouti, H.; Vivier, V.; Ziani, M., Electrochemical and spectroscopic characterizations of patinas formed on an archaeological bronze coin. Electrochimica Acta, 50 (**2005**) 24, 4699–4709

[23] Sidot, E.; Souissi, N.; Bousselmi, L.; Triki, E.; Robbiola, L., Study of the corrosion behaviour of Cu–10Sn bronze in aerated Na2SO4 aqueous solution. Corrosion Science, 48 (**2006**) 8, 2241–2257

[24] Strandberg, H., Reactions of copper patina compounds–II. influence of sodium chloride in the presence of some air pollutants. Atmospheric Environment, 32 (**1998**) 20, 3521–3526

[25] Strandberg, H., Reactions of copper patina compounds–I. Influence of some air pollutants. Atmospheric Environment, 32 (**1998**) 20, 3511–3520

[26] Strehblow, H. H.; Titze, B., The investigation of the passive behaviour of copper in weakly acid and alkaline solutions and the examination of the passive film by esca and ISS. Electrochimica Acta, 25 (**1980**) 6, 839–850

[27] Varvara, S.; Muresan, L. M.; Rahmouni, K.; Takenouti, H., Evaluation of some non–toxic thiadiazole derivatives as bronze corrosion inhibitors in aqueous solution. Corrosion Science, 50 (**2008**) 9, 2596–2604

[28] Watanabe, M.; Toyoda, E.; Handa, T.; Ichino, T.; Kuwaki, N.; Higashi, Y.; Tanaka, T., Evolution of patinas on copper exposed in a suburban area. Corrosion Science, 49 (**2007**) 2, 766–780